Resource

Cell Host & Microbe

Global Analysis of Palmitoylated Proteins in *Toxoplasma gondii*

Graphical Abstract

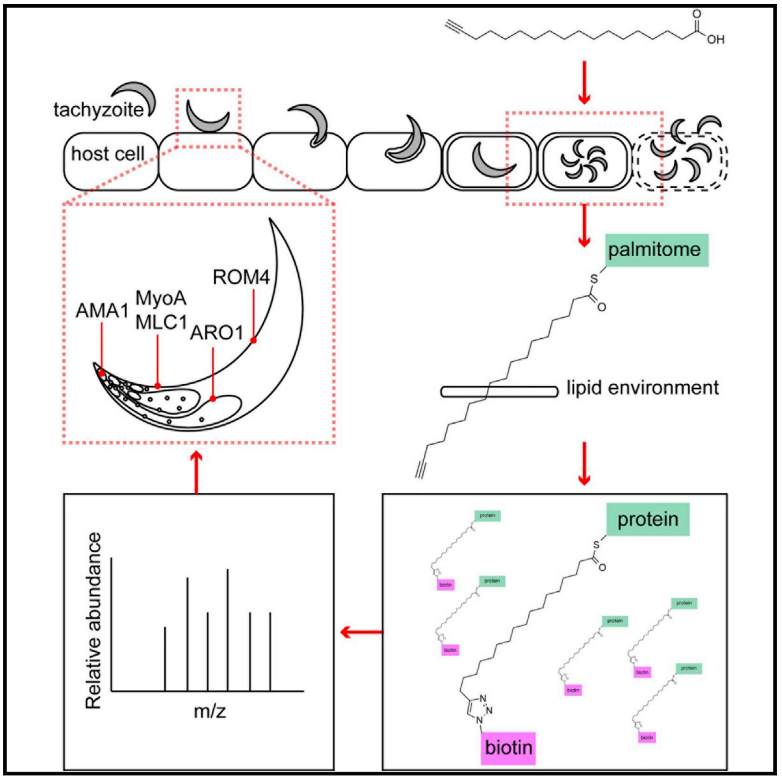

Authors

Ian T. Foe, Matthew A. Child, Jaimeen D. Majmudar, ..., Gary E. Ward, Brent R. Martin, Matthew Bogyo

Correspondence

brentrm@umich.edu (B.R.M.), mbogyo@stanford.edu (M.B.)

In Brief

Palmitoylation is a lipid-derived post-translational modification (PTM). Foe et al. report a comprehensive analysis of palmitoylated proteins in *Toxoplasma gondii*. They demonstrate that palmitoylation is associated with diverse aspects of *T. gondii* biology, including motility and morphology, and reveal a function for this PTM in regulating the invasion-associated protein, AMA1.

Highlights

- A Metabolic labeling approach was used to map the palmitome in *Toxoplasma gondii*
- Palmitoylation in *T. gondii* tachyzoites is highly prevalent
- Many components of the parasite's motility complex (glideosome) are palmitoylated
- AMA1 is palmitoylated, and its palmitoylation regulates microneme secretion

Foe et al., 2015, Cell Host & Microbe *18*, 501–511
October 14, 2015
http://dx.doi.org/10.1016/j.chom.2015.09.006

CellPress

Cell Host & Microbe
Resource

Global Analysis of Palmitoylated Proteins in *Toxoplasma gondii*

Ian T. Foe,[1,5] Matthew A. Child,[1,5] Jaimeen D. Majmudar,[2,5] Shruthi Krishnamurthy,[3] Wouter A. van der Linden,[1] Gary E. Ward,[3] Brent R. Martin,[2,*] and Matthew Bogyo[1,4,*]
[1]Department of Pathology, Stanford University School of Medicine, Stanford, CA 94305, USA
[2]Department of Chemistry, University of Michigan, Ann Arbor, MI 48109, USA
[3]Department of Microbiology and Molecular Genetics, University of Vermont, Burlington, VT 05405, USA
[4]Department of Microbiology and Immunology, Stanford University School of Medicine, Stanford, CA 94305, USA
[5]Co-first author
*Correspondence: brentrm@umich.edu (B.R.M.), mbogyo@stanford.edu (M.B.)
http://dx.doi.org/10.1016/j.chom.2015.09.006

SUMMARY

Post-translational modifications (PTMs) such as palmitoylation are critical for the lytic cycle of the protozoan parasite *Toxoplasma gondii*. While palmitoylation is involved in invasion, motility, and cell morphology, the proteins that utilize this PTM remain largely unknown. Using a chemical proteomic approach, we report a comprehensive analysis of palmitoylated proteins in *T. gondii*, identifying a total of 282 proteins, including cytosolic, membrane-associated, and transmembrane proteins. From this large set of palmitoylated targets, we validate palmitoylation of proteins involved in motility (myosin light chain 1, myosin A), cell morphology (PhIL1), and host cell invasion (apical membrane antigen 1, AMA1). Further studies reveal that blocking AMA1 palmitoylation enhances the release of AMA1 and other invasion-related proteins from apical secretory organelles, suggesting a previously unrecognized role for AMA1. These findings suggest that palmitoylation is ubiquitous throughout the *T. gondii* proteome and reveal insights into the biology of this important human pathogen.

INTRODUCTION

The phylum *Apicomplexa* is composed of medically relevant parasites, including *Plasmodium falciparum* and *Toxoplasma gondii*, the causative agents of malaria and toxoplasmosis, respectively. *T. gondii* is an obligate intracellular parasite that infects approximately 30% of the world's population (Robert-Gangneux and Dardé, 2012). The majority of infections are latent, asymptomatic, and maintained indefinitely inside the host as bradyzoite cysts. If an infected person becomes immunocompromised, cyst activation can cause acute toxoplasmosis, the symptoms of which include blindness and neurological problems (Montoya and Liesenfeld, 2004; Robert-Gangneux and Dardé, 2012). The *T. gondii* asexual lytic cycle comprises several distinct processes, including host cell invasion, intracellular replication, and egress (Black and Boothroyd, 2000). Completion of this cycle by tachyzoite-stage parasites is essential for parasite survival within a host, and a better understanding of these processes is prerequisite for the development of therapies to combat infection.

Recent work has implicated the post-translational modification (PTM) S-palmitoylation as being important for the tachyzoite lytic cycle (Alonso et al., 2012). S-palmitoylation is the covalent attachment of palmitate (Figure 1A), a saturated 16-carbon fatty acid, via a thioester linkage to a cysteine residue (Linder and Deschenes, 2007; Tom and Martin, 2013). Palmitoylation typically regulates protein membrane localization, but can also alter protein stability, protein/protein interactions, and protein trafficking (Linder and Deschenes, 2007; Salaun et al., 2010). Unlike other lipid modifications, palmitoylation is reversible and dynamic (Martin et al., 2012). The addition of palmitate is catalyzed by palmitoyl acyl transferases (PATs) (Linder and Deschenes, 2007). The *T. gondii* genome encodes 18 potential PATs, 16 of which are expressed in tachyzoites (Frénal et al., 2013). There are two primary families of palmitoyl thioesterases: palmitoyl protein thioesterases, which remove palmitate from proteins found in lysosomes, and acyl-protein thioesterases (APTs), which target palmitoylated cytosolic proteins (Linder and Deschenes, 2007). The *T. gondii* genome is predicted to encode four APTs (Kemp et al., 2013), only one of which has confirmed thioesterase activity (Child et al., 2013).

A growing body of work has implicated palmitoylation in multiple aspects of *T. gondii* biology. Treating tachyzoites with the broadly reactive PAT inhibitor, 2-bromopalmitate (2-BP), inhibits motility and host cell invasion and disrupts parasite morphology (Alonso et al., 2012). Similarly, 2-BP treatment of blood-stage *P. falciparum* inhibits invasion and alters parasite morphology (Jones et al., 2012). Inhibition of a *T. gondii* APT (TgPPT1) results in increased motility and invasion (Child et al., 2013). Despite the importance of palmitoylation in the *T. gondii* asexual life cycle, only five proteins have been definitively shown to be palmitoylated, with mutational studies suggesting that eight others likely have this PTM (Table 1). The full extent of protein palmitoylation in *T. gondii* remains largely unknown and likely regulates many aspects of parasite biology.

To understand the extent and function of palmitoylation in *T. gondii* tachyzoite biology, we undertook a chemical proteomic study to profile the full complement of palmitoylated proteins in

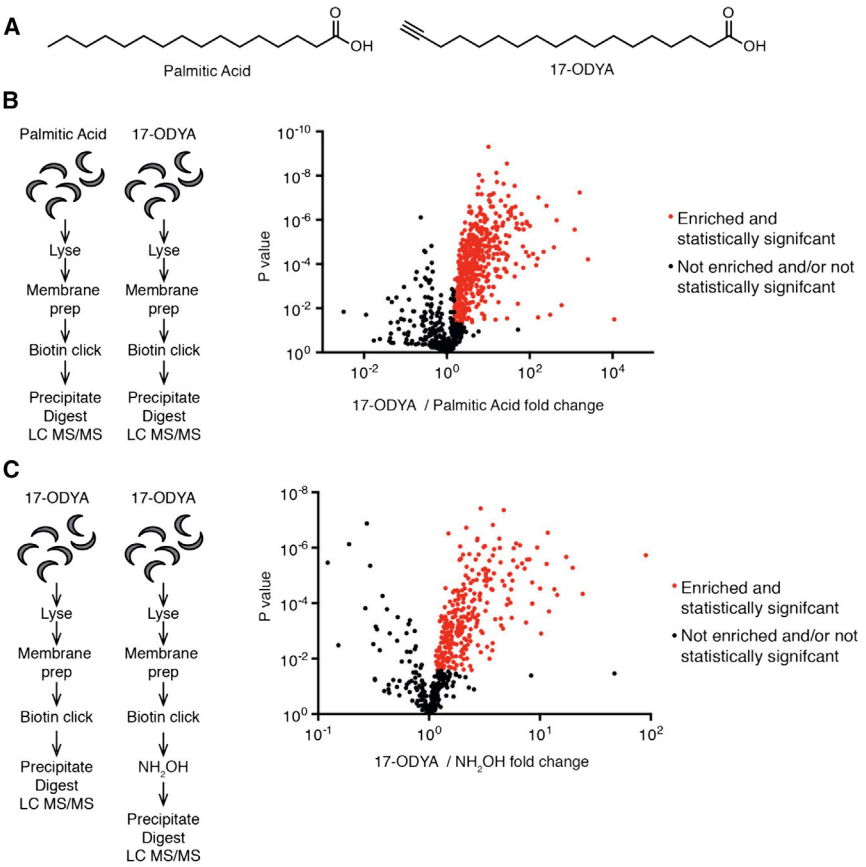

Figure 1. Identification of Palmitoylated Proteins in *T. gondii* Tachyzoites

(A) Chemical structure of palmitic acid and 17-octadecynoic acid (17-ODYA).

(B) Left, diagram of approach to identify palmitoylated proteins. Right, ratio of average normalized abundance scores of proteins isolated from 17-ODYA-treated parasites over average normalized abundance in palmitic acid-treated parasites (834 proteins), plotted against statistical significance. Red dots are proteins with a fold change (17-ODYA abundance/palmitic acid abundance) of $\geq$1.5 ($p < 0.05$) and that satisfied 5% FDR (501 proteins). Black dots are proteins with a fold change of <1.5 and/or not statistically significant ($p > 0.05$) and/or did not satisfy 5% FDR.

(C) Left, diagram of approach to identify 17-ODYA-labeled proteins sensitive to hydroxylamine. Right, ratio of average normalized abundance scores of proteins isolated in 17-ODYA-treated samples over average normalized abundance score of proteins isolated from 17-ODYA treated samples that were then treated with hydroxylamine, plotted against statistical significance (501 proteins identified above). Red dots are proteins (282 proteins) with a fold change (average 17-ODYA abundance/average hydroxylamine abundance) of $\geq$1.0 ($p < 0.05$) and that satisfy 5% FDR. Black dots are proteins with a fold change of <1 and/or not statistically significant ($p > 0.05$) and/or did not satisfy 5% FDR. See also Figure S1 and Table S1.

T. gondii tachyzoites. These efforts identified proteins involved in a variety of biological processes, including host cell invasion, motility, morphology, signaling, stress response, and metabolism. We biochemically confirm the palmitoylation of several candidates from our proteomic analysis, including myosin light chain 1 (MLC1) and myosin A (MyoA), components of the glideosome, the parasite's motility complex (Herm-Götz et al., 2002; Meissner et al., 2002). We confirm that the morphology-associated photosensitized INA-labeled protein (PhIL1) (Barkhuff et al., 2011; Gilk et al., 2006) is palmitoylated. Unexpectedly, we found that apical membrane antigen 1 (AMA1), a protein that functions during invasion (Hehl et al., 2000; Lamarque et al., 2014; Mital et al., 2005), is palmitoylated. Mutation of the identified palmitoylation site has no effect on invasion or protein localization but markedly enhances microneme secretion and affects the ability of parasites to complete the intracellular stages of the lytic cycle. Combined, these findings reveal a valuable dataset that will help to drive the discovery of specific functional roles for palmitoylation in *T. gondii* tachyzoite biology.

RESULTS

Identification of Palmitoylated Proteins by Mass Spectrometry

There have been a number of recent technological advances in the use of chemical tools to study lipidated proteins (Hang et al., 2007; Hannoush and Arenas-Ramirez, 2009; Heal et al., 2008; Kostiuk et al., 2008; Martin and Cravatt, 2009). This includes the development of methods to apply the palmitic acid analog 17-octadecynoic acid (17-ODYA) as a bioorthogonal tag to identify palmitoylated proteins (Figure 1A) (Jones et al., 2012; Martin and Cravatt, 2009). This palmitate mimetic contains a terminal alkyne for "Click" reaction (copper-catalyzed cycloaddition) with azide-containing molecules such as biotin (for affinity enrichment), or rhodamine (for in-gel visualization by SDS-PAGE) (Martin and Cravatt, 2009). We have previously used 17-ODYA to metabolically label *T. gondii* tachyzoites for direct detection of specific palmitoylated proteins (Child et al., 2013). We therefore applied this method more broadly to globally profile palmitoylation in *T. gondii*.

To ensure complete analysis of all palmitoylated proteins, we first determined the kinetics of labeling by 17-ODYA. We observed metabolic incorporation of 17-ODYA on proteins within 1 hr of incubation, with labeling saturated by 16 hr (Figure S1A). We then treated parasites for 16 hr with a range of concentrations of 17-ODYA to determine the optimal concentration to use for our proteomic studies (Figure S1B). We chose a concentration of 25 μM as it gave robust and consistent labeling, was not toxic (Figure S1C), and was the concentration used for prior human and *P. falciparum* palmitoylation studies (Jones et al., 2012; Martin and Cravatt, 2009). For our proteomic workflow, we metabolically labeled wild-type tachyzoites (RH strain) with either 17-ODYA or palmitic acid for 16 hr, sonicated the parasites, and fractionated the resulting material into soluble and

Table 1. Proteins with Prior Experimental Evidence of Palmitoylation

Protein	Previous Evidence of Palmitoylation	Identified	Highly NH_2OH Sensitive	NH_2OH Fold Change
GAP45	Frénal et al., 2010 Child et al., 2013	Yes	Yes	5.8
CDPK3	Lourido et al., 2012 McCoy et al., 2012 Garrison et al., 2012 Child et al., 2013	Yes	No	1.4
ARO	Beck et al., 2013 Mueller et al., 2013 Child et al., 2013	Yes	Yes	2
HSP20	De Napoli et al., 2013	Yes	Yes	3.4
HXGPRT	Chaudhary et al., 2005	Yes	Yes	3.2
MLC1	Frénal et al., 2010	Yes	Yes	3.1
MLC2	Polonais et al., 2011	Yes	Yes	5.6
IAP1	Frénal et al., 2014	Yes	Yes	2.6
GAP70	Frénal et al., 2010	No	–	–
ISP1	Beck et al., 2010	No	–	–
ISP2	Beck et al., 2010	Yes	No	1.1
ISP3	Beck et al., 2010	Yes	Yes	1.8
ISP4	Fung et al., 2012	No	–	–

Hydroxylamine sensitivity (NH_2OH) in the current study is shown, with fold change after NH_2OH treatment indicated.

insoluble fractions. Previous studies employing this approach have not observed significant 17-ODYA-dependent labeling of soluble proteins (Martin and Cravatt, 2009), and we focused on insoluble proteins for the remainder of the study. Accordingly, this study does not include analysis of potentially soluble palmitoylated proteins. After chloroform/methanol precipitation, we performed click conjugation of azido-biotin in the insoluble membrane fraction and collected labeled proteins by streptavidin enrichment. Following trypsin digestion, we analyzed the peptides by 1D reverse-phase nanoUPLC coupled to a quadrupole ion mobility time of flight mass spectrometer. We acquired data using UDMS^E methods (Distler et al., 2014) for label-free data-independent acquisition (DIA). In this approach, data are collected across the entire mass range, cycling between low collision energy (precursors) and high collision energy (products), recording data for all precursor and product ions across the entire elution gradient. After multi-dimensional alignment by drift and elution times, precursor ions are matched to product ions for database annotation using a 1% reverse-decoy false discovery rate (FDR). Leveraging this DIA approach, we extracted ion intensities for each annotated peptide across each 1D experiment (four biological replicates, each the average of three technical replicates) and normalized each dataset to pyruvate carboxylase, an endogenous biotinylated protein. This approach yielded statistically robust, reproducible, label-free quantitation with no gaps in data across experiments. In control experiments using a standard HeLa digest (n = 4), the technical error was approximately 17% (SD), ensuring statistically significant quantitation of as little as 35% changes (2 SD) (Figure S1D). Based on slightly more stringent thresholds, we identified and quantified 501 *T. gondii* proteins statistically enriched ($p < 0.05$, >1.5-fold, 5% FDR) in 17-ODYA relative to the palmitic acid control (Figure 1B, Table S1).

In addition to reversible S-palmitoylation, palmitate can be irreversibly attached to the hydroxyl group of serine residues (O-palmitoylation) (Zou et al., 2011) and to the amine group on N-terminal cysteines (N-palmitoylation) (Linder and Deschenes, 2007). It can also be irreversibly incorporated into glycosylphosphatidylinositol (GPI) anchors such as on *T. gondii*, Subtilisin 1 (SUB1) (Binder et al., 2008). Consistent with this, SUB1 was highly enriched in 17-ODYA samples (Table S1). Therefore, to focus S-palmitoylated proteins, we performed a second proteomic experiment where we treated samples with hydroxylamine to hydrolyze any thioester linkages (Figure 1C). Following label-free DIA analysis, we confirmed statistically significant ($p < 0.05$) hydroxylamine hydrolysis for 282 proteins (Figure 1C, Table S1), 210 of which were enriched >1.5-fold in the untreated sample (highly hydroxylamine sensitive) and 72 of which were enriched between 1- and 1.5-fold (sensitive). These 282 proteins represent our final list of *T. gondii* palmitoylated proteins. (Figure 2A, Table S1). Importantly, this included 9 of the 13 established palmitoylated proteins in our data (Table 1), suggesting that the method was sufficiently robust to annotate the vast majority of palmitoylated proteins. We predict this is an underrepresentation of the number of *T. gondii* palmitoylated proteins, as our analysis did not use extensive fractionation and focused on a single life cycle stage. Nonetheless, the high statistical confidence provides a broad profile of thioester-dependent 17-ODYA labeling in *T. gondii*.

We next assessed how palmitoylation may be involved in distinct aspects of the parasite asexual biology and found that our dataset contained proteins involved in all aspects of the lytic cycle (Figure 2B). In addition, we found that 37% of the highly hydroxylamine-sensitive proteins and 19% of sensitive proteins were annotated as hypothetical (Figure 2C). Consistent with reports that palmitoylation often occurs proximal to or within transmembrane (TM) domains (Charollais and Van Der Goot, 2009), we found that TM domain-containing proteins were enriched in the highly hydroxylamine-sensitive proteins in our dataset (37%) compared to a *T. gondii* membrane proteome (30%) (Che et al., 2011) and the predicted *T. gondii* proteome (20%) (Figure 2C). In addition to TM domains, mammalian palmitoylation is enriched at cysteine residues close to the N terminus of a protein when glycine is the second amino acid, which are frequently myristoylated. Our dataset was not significantly enriched for proteins with glycine in the second position, as 7%–8% of the proteins in our data had a glycine in this position, compared to the *T. gondii* membrane proteome (7%) (Che et al., 2011) and the predicted proteome (6%) (Figure 2C). This lack of enrichment may be an artifact of how we set our selection criteria, as dually acylated proteins may be less sensitive to hydroxylamine treatment.

Recent proteomic studies have defined the *P. falciparum* palmitome (Jones et al., 2012). Due to the relatedness of these two organisms, we compared the *P. falciparum* palmitome and our *T. gondii* dataset, helping us validate likely palmitoylation events and identify modifications unique to either parasite. We initially converted the entire *P. falciparum* palmitome dataset (Jones et al., 2012) into putative *T. gondii* orthologs. This analysis

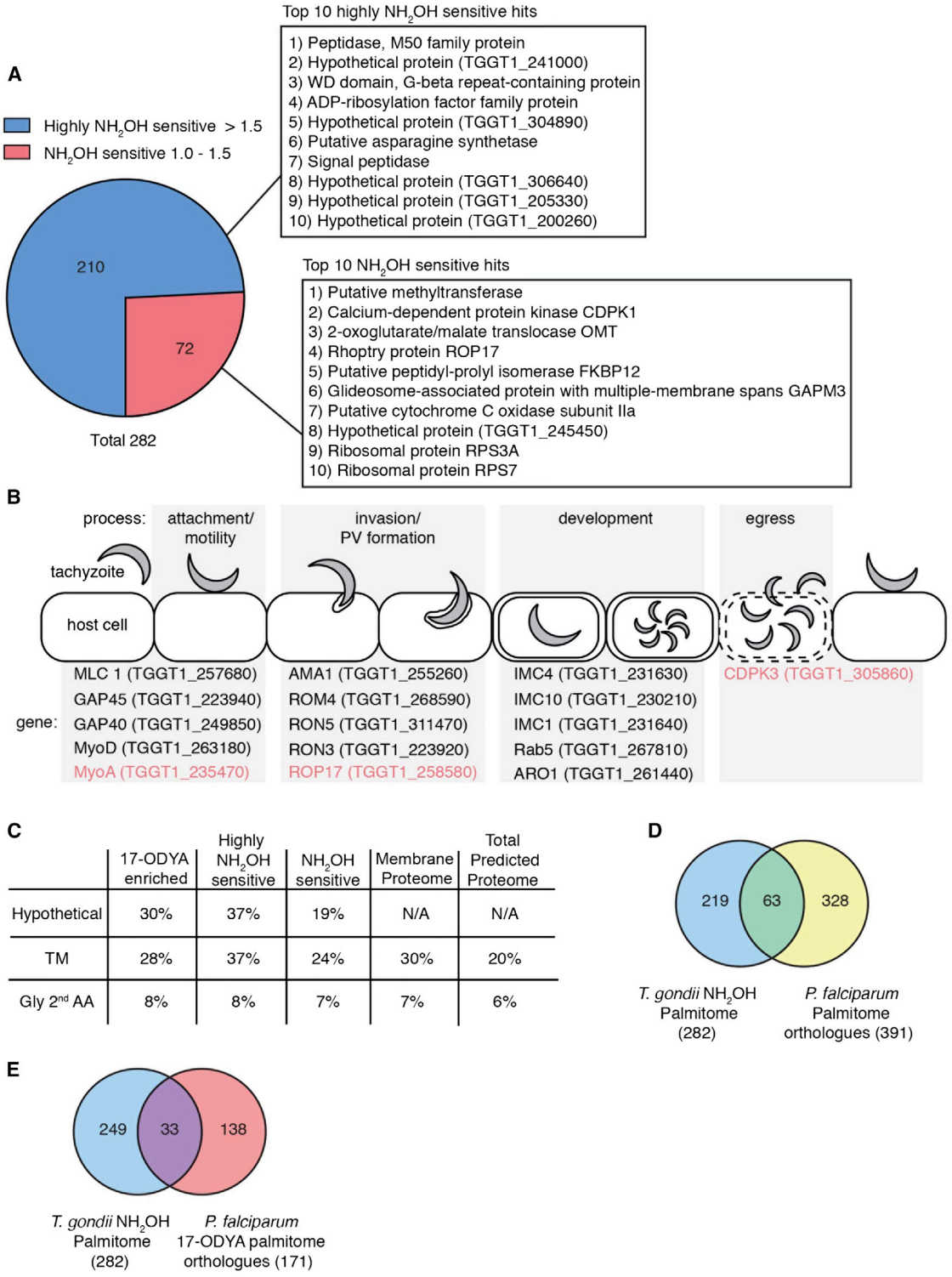

	17-ODYA enriched	Highly NH_2OH sensitive	NH_2OH sensitive	Membrane Proteome	Total Predicted Proteome
Hypothetical	30%	37%	19%	N/A	N/A
TM	28%	37%	24%	30%	20%
Gly 2nd AA	8%	8%	7%	7%	6%

Figure 2. Analysis of MS Data

(A) Pie chart depicting 282 proteins identified as putatively S-palmitoylated. Confidence intervals for hydroxylamine (NH_2OH) sensitivity are indicated (highly hydroxylamine sensitive >1.5 [blue], hydroxylamine sensitive 1.0–1.5 [red]). Total numbers of proteins in each interval are shown, as are the identities of the top 10 hits for both confidence levels.

(B) Proteins implicated in diverse functions are palmitoylated in *T. gondii* tachyzoites. Gene names and accession numbers are provided for a subset of proteins from the MS dataset that highlight the diversity of palmitoylated proteins found. Black text is used to indicate palmitoylated proteins highly sensitive to hydroxylamine, and red text indicates hydroxylamine-sensitive hits.

(legend continued on next page)

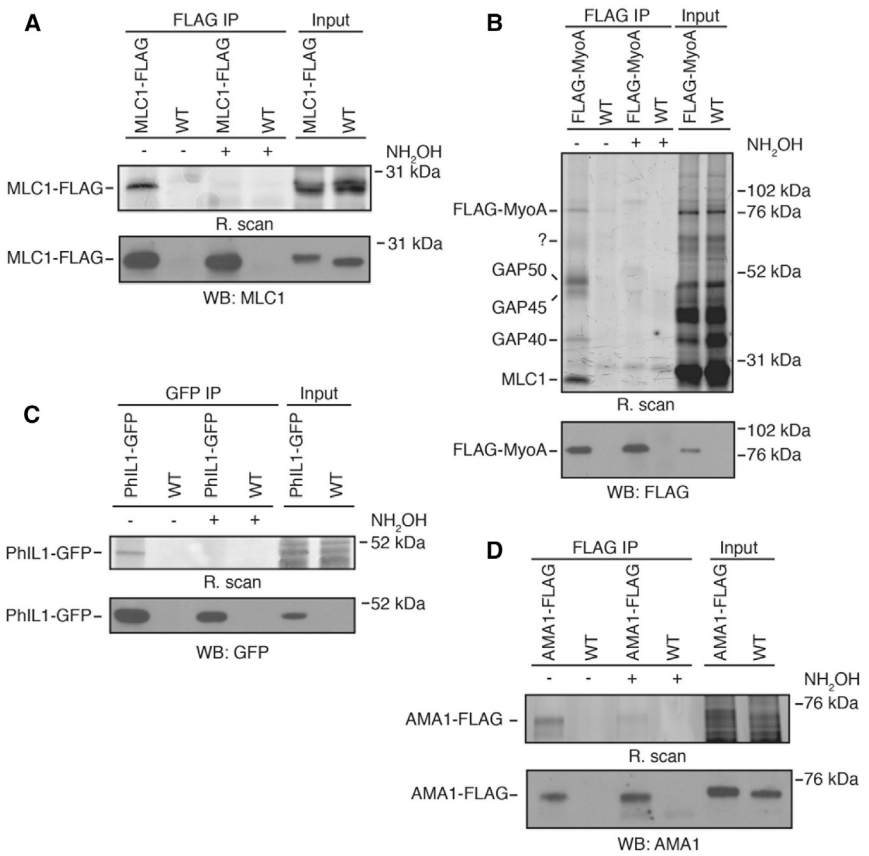

Figure 3. Validation of a Subset of Palmitoylated Proteins

In all cases, treatment with 5% hydroxylamine is indicated by ±NH_2OH.

(A) MLC1-FLAG IP showing that MLC1 is palmitoylated. Top: rhodamine fluorescent scan (R. scan) of SDS-PAGE showing palmitoylation of MLC1. Bottom: corresponding western blot for MLC1-FLAG IP, probed with anti-MLC1 antibody (WB: MLC1).

(B) FLAG-MyoA IP showing that MyoA is palmitoylated. Top: rhodamine fluorescent scan (R. Scan) of SDS-PAGE showing palmitoylation of MyoA. Co-precipitating species are tentatively assigned identities based on electrophoretic mobility and indicated on gel. Bottom: corresponding western blot of FLAG-MyoA IP, probed with anti-FLAG antibody (WB: FLAG).

(C) PhIL1-GFP IP showing palmitoylation of PhIL1. Top: rhodamine fluorescent scan (R. scan) of SDS-PAGE showing palmitoylation of PhIL1. Bottom: corresponding western blot for PhIL1-GFP, probed with anti-GFP antibody (WB: GFP).

(D) AMA1-FLAG IP showing palmitoylation of AMA1. Top: rhodamine fluorescent scan (R. scan) of SDS-PAGE showing palmitoylation of AMA1. Bottom: corresponding western blot for AMA1 IP, probed with anti-AMA1 antibody (WB: AMA1) See also Figure S2.

identified 391 *T. gondii* orthologs corresponding to 313 of the 494 *P. falciparum* proteins. Of these, 63 were shared between our data and the entire *P. falciparum* palmitome (Figure 2D, Table S2). We also observed limited overlap between our data and the 17-ODYA-generated *P. falciparum* palmitome (Figure 2E, Table S2). The overlap between the datasets was unexpectedly small, which could be due to substantial differences in the way the two parasites use palmitoylation, overall poor homology between palmitoylated proteins in these parasites, or that different life cycle stages are being compared, i.e., intracellular *P. falciparum* schizonts and extracellular *T. gondii* tachyzoites.

Validation of Protein Palmitoylation

To confirm that proteins identified in our proteomic analysis were in fact palmitoylated, we carried out direct validation studies in which specific proteins from our dataset were isolated by immunoprecipitation and the presence of the palmitate analog (17-ODYA) confirmed biochemically. MLC1 was previously suggested to be palmitoylated (Frénal et al., 2010). We metabolically labeled MLC1-FLAG-expressing parasites (Leung et al., 2014) with 17-ODYA, immunoprecipitated MLC1 with the FLAG epitope, used Click chemistry to attach an azido-rhodamine fluorophore, and analyzed the labeled proteins by SDS-PAGE (Figure 3A). We observed a strong fluorescent signal associated with MLC1, which was reduced by hydroxylamine treatment. These results are consistent with the MS data and confirm that MLC1 is palmitoylated in tachyzoites.

We also identified the MLC1-binding partner MyoA as being putatively palmitoylated in our dataset. We metabolically labeled parasites expressing an N-terminal FLAG-tagged MyoA (Tang et al., 2014) with 17-ODYA. Using the FLAG epitope, we immunoprecipitated MyoA and then labeled with azido-rhodamine. We observed a fluorescent signal associated with MyoA by SDS-PAGE that was lost by treatment with hydroxylamine (Figure 3B), indicating that MyoA is genuinely palmitoylated. In addition to the rhodamine signal observed for MyoA, we detected fluorescent signals from five other protein species that co-precipitated with MyoA that were similarly hydroxylamine sensitive (Figure 3B). Interestingly, the pattern of co-precipitating

(C) Table shows hypothetical proteins (Hypothetical), proteins with predicted transmembrane domains (TM), and proteins with a glycine as the second amino acid (Gly 2nd AA) expressed as a percentage of the total number of proteins from the following datasets: 17-ODYA enriched, highly hydroxylamine sensitive and sensitive hits, membrane proteome, and the total predicted coding sequences in the genome (Total Predicted Proteome).

(D) Venn diagram showing overlap between the entire *P. falciparum* palmitome and the *T. gondii* palmitome. Left circle (blue) represents the *T. gondii* palmitome. Right circle (yellow) are the orthologs within the *P. falciparum* palmitome. Overlap (green) shows proteins identified in both datasets. Numbers indicate the number of proteins identified.

(E) Venn diagram showing overlap between the 17-ODYA *P. falciparum* palmitome and the *T. gondii* palmitome. Left circle (blue) represents the *T. gondii* palmitome. Right circle (red) are the orthologs within the *P. falciparum* 17-ODYA palmitome. Overlap (purple) shows proteins identified in both datasets. Numbers are the number of proteins identified. See also Tables S1 and S2.

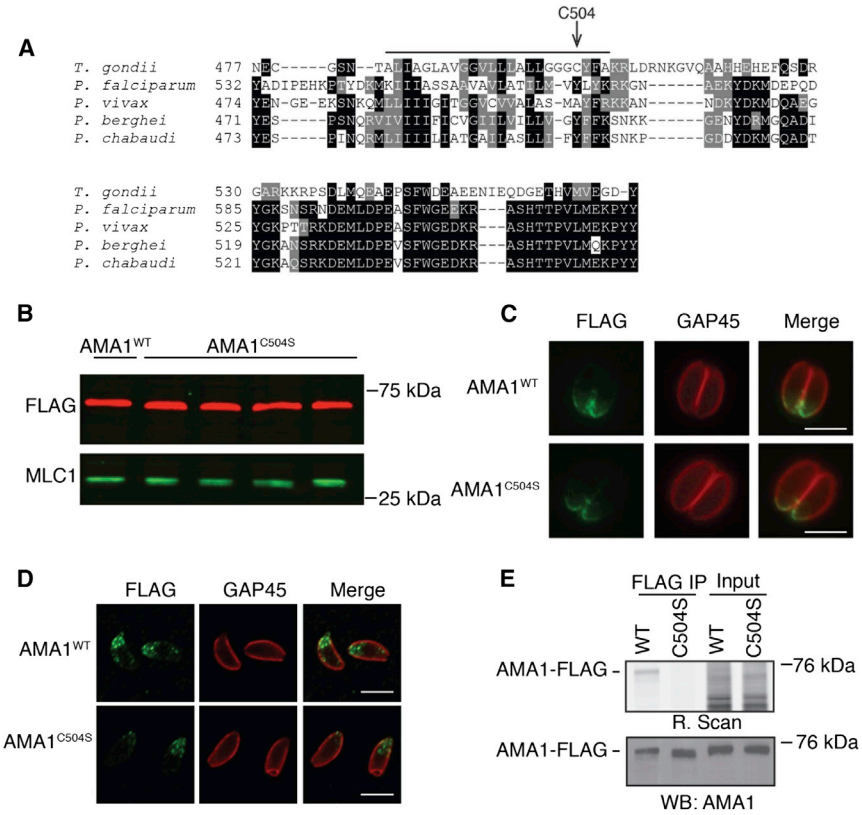

Figure 4. AMA1 Is Palmitoylated at Cysteine 504

(A) Alignment of the transmembrane domain and flanking residues of *T. gondii* AMA1 with the corresponding region of AMA1 from several *Plasmodium* species. Arrow indicates cysteine 504; line indicates predicted transmembrane in *T. gondii* AMA1. Shading indicates conservation: black for good, gray for average, white for non.

(B) Western blot for AMA1^{WT} and four AMA1^{C504S} clones showing that AMA1^{C504S} is expressed at similar levels as AMA1^{WT}. MLC1, loading control.

(C) Immunofluorescence microscopy of AMA1^{WT} and AMA1^{C504S} intracellular parasites. AMA1-FLAG staining is shown in green. GAP45 staining is shown in red. Scale bar, 5 μm.

(D) Immunofluorescence microscopy of AMA1^{WT} and AMA1^{C504S} extracellular parasites. AMA1-FLAG staining is shown in green. GAP45 staining is shown in red. Scale bar, 5 μm.

(E) AMA1-FLAG IP showing that Cys504 is necessary for AMA1 palmitoylation. Top: rhodamine fluorescent scan (R. scan) of SDS-PAGE showing signal only in AMA1^{WT} lane. Bottom: corresponding western blot for AMA1 IP, probed with anti-AMA1 antibody showing amount of AMA1 immunoprecipitated (WB: AMA1). See also Figure S3.

proteins resembled the profile previously identified as the core components of the glideosome (Frénal et al., 2010; Gaskins et al., 2004). Given literature reports and the electrophoretic mobility of the protein species, we tentatively annotated them as GAP45 (a confirmed palmitoylated protein (Child et al., 2013; Frénal et al., 2010), MLC1 (shown in this study to be palmitoylated), GAP40, and GAP50 (Figure 3B). However, without MS identification of these MyoA-associated proteins we cannot conclusively confirm their identity. GAP40 and GAP50 have not previously been reported to be palmitoylated, but our proteomic data indicated that they likely are, with GAP40 labeling being highly hydroxylamine sensitive and GAP50 hydroxylamine sensitive. We also observed a faint diffuse protein species between 50 and 70 kDa that was specific to the IP and also hydroxylamine sensitive (Figure 3B). While the identity of this protein has yet to be confirmed, based on a recent description of alternative glideosome complexes, we believe that this protein is likely either GAP70 or GAP80 (Frénal et al., 2014; Frénal et al., 2010). Consistent with this assignment, GAP80 is present as a highly hydroxylamine-sensitive hit in our dataset. Therefore, our data suggest that the glideosome is a heavily palmitoylated complex in tachyzoites.

Inhibition of palmitoylation has been shown to disrupt parasite morphology (Alonso et al., 2012). Consistent with this, our chemical proteomic approach identified PhIL1, which has been previously implicated in parasite morphology (Barkhuff et al., 2011), as being palmitoylated. We metabolically labeled parasites expressing a GFP-tagged PhIL1 (Gilk et al., 2006) with 17-ODYA. We immunoprecipitated PhIL1 and performed a click reaction with azido-rhodamine, observing a fluorescent signal that was lost upon hydroxylamine treatment, confirming that PhIL1 is also palmitoylated (Figure 3C).

AMA1 Is Palmitoylated

Identification of the invasion-associated protein AMA1 (Donahue et al., 2000; Hehl et al., 2000; Lamarque et al., 2014; Mital et al., 2005) as one of the highly hydroxylamine sensitive hits in our dataset was intriguing, as palmitoylation has been implicated in the regulation of host cell invasion (Alonso et al., 2012; Child et al., 2013). We labeled parasites expressing FLAG-tagged AMA1 (Parussini et al., 2012) with 17-ODYA, immunoprecipitated AMA1 using the FLAG epitope, and labeled with azido-rhodamine. We observed a strong fluorescent signal for AMA1 isolated from both extracellular (Figure 3D) and intracellular parasites (Figure S2), which was greatly reduced by hydroxylamine treatment, indicating that AMA1 is palmitoylated.

We next sought to identify the site of palmitoylation on AMA1, which contains 18 cysteine residues (Donahue et al., 2000; Hehl et al., 2000). Structural studies indicate that 16 of these cysteines form disulfide bridges in the protein's extracellular domain and are therefore not likely to be sites of palmitoylation (Crawford et al., 2010). One of the remaining two cysteines lies within a predicted signal peptide, which is not expected to be part of the mature protein (Donahue et al., 2000; Hehl et al., 2000). The remaining cysteine is located at position 504 in the C-terminal end of the predicted TM domain, proximal to the cytosol-exposed tail region (Figure 4A). This particular cysteine is not conserved in *P. falciparum* and other related *Plasmodium* species, although several *Plasmodium* species contain cysteines

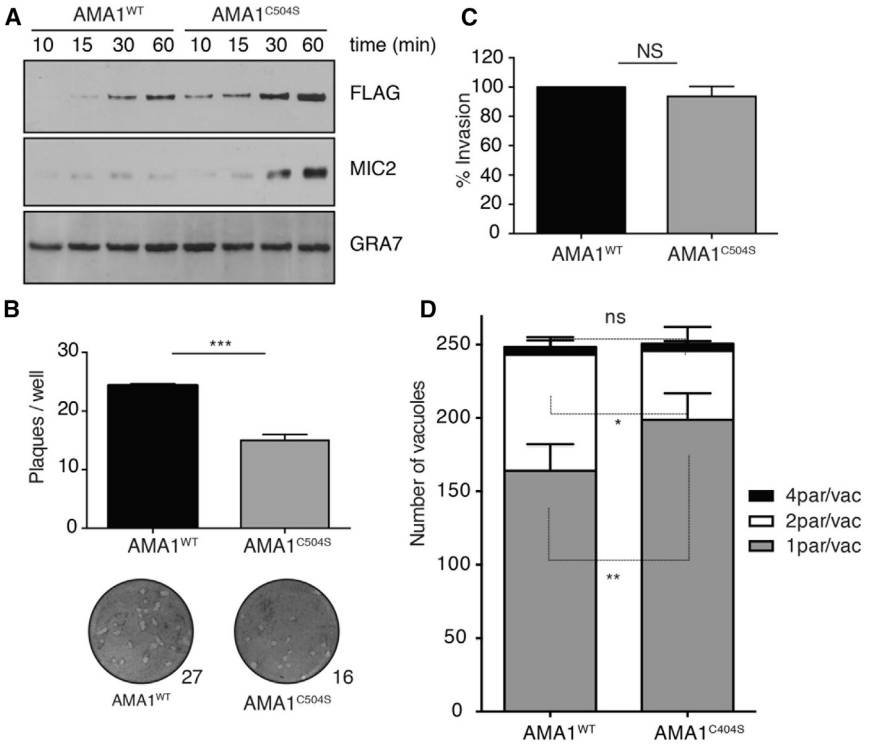

Figure 5. Phenotypic Analysis of AMA1^{C504S} Strain

(A) Secretion of AMA1 and MIC2 is increased in AMA^{C504S} parasites. Anti-FLAG blot of the assay supernatant shows the rate of constitutive AMA1 secretion, and the MIC2 blot shows the rate of constitutive MIC2 secretion. GRA7 recovered in the assay supernatant was used as a control.

(B) AMA1^{C504S} parasites generate ~40% fewer plaques. Top, histogram of quantification of plaque assays for AMA1^{WT} and AMA1^{C504S}. Each bar shows the mean of three biological replicates, each performed in technical triplicate. Error bars indicate SEM, calculated using two-tailed Student's t test (***p = 0.0009). Bottom, representative images of plaque assays comparing AMA1^{WT} and AMA1^{C504S} growth. Number of plaques is indicated in the bottom right corner.

(C) AMA1^{C504S} parasites invade host cells normally. Histogram presents quantification of three independent invasion assays. Percent invasion shown for AMA1^{C504S} relative to AMA1^{WT} invasion. Error bars indicate SD; NS, not significant.

(D) AMA1^{C504S} is defective at transitioning from one parasite/vacuole to two parasites/vacuole after being extracellular for 4 hr. Histogram presents quantification of three independent replication assays. Number of parasites/parasitophorous vacuole is indicated. Significance was calculated using Sidak's multiple comparisons test (**p = 0.0092, *p = 0.019). Error bars denote SD. See also Figure S4.

at other positions within their TM domains (Figure 4A). PfAMA1, which lacks this cysteine, was not identified in the *P. falciparum* palmitome (Jones et al., 2012).

To determine if Cys504 was required for TgAMA1 palmitoylation, we generated parasite strains in which endogenous *AMA1* was replaced with either wild-type (WT) FLAG-tagged allele (*AMA1^{WT}*) or a FLAG-tagged allele containing a Cys504Ser mutation (*AMA1^{C504S}*; Figure S3). AMA1^{C504S} parasites were viable and expressed AMA1^{C504S} at steady-state levels equivalent to those of AMA1^{WT} (Figure 4B). The localization of AMA1^{C504S} was indistinguishable from AMA1^{WT} in intracellular (Figure 4C) and extracellular parasites (Figure 4D): staining was detectable around the entire periphery of the parasite and concentrated at the apical end, as previously described (Donahue et al., 2000; Hehl et al., 2000). We metabolically labeled both AMA1^{WT} and the AMA1^{C504S} strains with 17-ODYA, immunoprecipitated AMA1 using the FLAG epitope, and labeled with azido-rhodamine. AMA1^{WT} yielded a strong fluorescent signal visualized by SDS-PAGE, whereas the AMA1^{C504S} showed no detectable rhodamine fluorescence (Figure 4E). These data strongly suggest that residue Cys504 is essential for, and likely the site of, palmitoylation on AMA1.

Following secretion from the micronemes to the parasite plasma membrane, AMA1 is cleaved within its TM domain by the rhomboid protease ROM4 (Rugarabamu et al., 2015; Shen et al., 2014), and its ectodomain is released from the parasite. As Cys504 lies within the AMA1 TM domain, we hypothesized that palmitoylation on this site might regulate AMA1 intramembrane cleavage and shedding. Microneme secretion assays, which measure the combined effect of secretion to the parasite surface and intramembrane proteolysis, revealed a striking increase in the amount of AMA1^{C504S} ectodomain released in the culture supernatant compared to AMA1^{WT} (Figures 5A and S4C). Surprisingly, a similar increase was observed for the shedding of the microneme protein 2 (MIC2) in the AMA1^{C504S} parasites (Figure 5D), suggesting that AMA1 palmitoylation influences the rate of microneme secretion. Secretion of a dense granule marker (GRA7) and rhoptry marker (ROP1) was unaffected (Figures 5A, S4C, and S4D), indicating that increased secretion in the mutant is restricted to micronemes and is not observed for other apical complex organelles.

In standard plaque assays, AMA1^{C504S} parasites consistently formed ~40% fewer plaques than AMA1^{WT}. However, the plaques that formed were of roughly equal size (Figure 5B), and the mutant parasites showed no detectable defect in invasion (Figure 5C). Since the mutant parasites formed fewer plaques but invaded normally, we tested whether the AMA1^{C504S} plaquing defect resulted from an inability to complete the intracellular phase of the lytic cycle. In initial replication assays with freshly egressed parasites, we observed no difference in parasite intracellular growth (data not shown). When the parasites were incubated extracellularly for 4–5 hr before addition to host cells, there was still no difference in the invasiveness of AMA1^{C504S} and AMA1^{WT} parasites (Figure S4E). However, a smaller percentage of the aged AMA1^{C504S} parasites that invaded were able to complete their intracellular replicative cycle compared to aged AMA1^{WT} parasites (Figure 5D), likely explaining the reduced number of plaques observed in the mutants despite their similar levels of invasion. Finally, recent studies have shown that in the absence of AMA1, parasites upregulate AMA2 as a

compensatory response (Lamarque et al., 2014). To investigate if a similar compensation had occurred, we compared the expression levels of AMA2 and AMA4 by qPCR in the wild-type and C504S mutant (Figures S4A and S4B). AMA4 expression levels were unchanged; however, there was a slight, but significant, downregulation of AMA2 in the mutant. The underlying biological significance and relationship to our phenotype remain to be determined.

DISCUSSION

S-palmitoylation is the post-translational addition of a saturated 16-carbon fatty acid onto proteins via cysteine thiols (Tom and Martin, 2013). Modern approaches enable proteome-wide identification of proteins modified by palmitate (Martin and Cravatt, 2009). These "palmitomes" have confirmed the presence of this PTM through diverse aspects of biology and across disparate branches of the tree of life. For example, a recent study defined the palmitome of the apicomplexan parasite, *P. falciparum*, concluding that palmitoylation plays a central role in regulating blood-stage development (Jones et al., 2012). Here, we applied a comprehensive DIA-MS chemoproteomic approach to study palmitoylation of a related apicomplexan parasite, *T. gondii*. Focusing on the asexual tachyzoite stage, we discovered that palmitate is incorporated onto proteins involved in all aspects of the tachyzoite lytic cycle, identifying the majority of proteins previously predicted to be palmitoylated in *T. gondii* (Table 1). Additionally, using a biochemical method developed in our previous study (Child et al., 2013), we validated our dataset and showed that multiple proteins not previously known to be palmitoylated are modified by this PTM.

Despite growing knowledge of specific sites of palmitoylation, recognition motifs that direct modification remain poorly defined (Linder and Deschenes, 2007; Salaun et al., 2010). It is not clear if the rules or motifs are evolutionarily conserved or if they are specific to a given organism of interest. CSS-Palm (http://csspalm.biocuckoo.org/) is open-source software that provides a bioinformatic prediction of the likelihood that a given cysteine will be palmitoylated (Ren et al., 2008). CSS-Palm 4.0 predicts with high confidence that approximately 56% percent (4,755/8,460) of the coding genes in *T. gondii* produce potentially palmitoylated proteins, compared with the 282 proteins identified in our dataset (3.3% of the coding sequences in the genome). Consistent with our data, CSS-Palm 4.0 predicts with high confidence that AMA1 is palmitoylated. However, the software identifies a cysteine within the predicted signal peptide of the molecule as the likely site of modification, not Cys504, which we identified as the likely site of palmitoylation. Our findings indicate that caution should be exercised when using bioinformatic approaches to identify palmitoylated proteins.

In this study, we present the use of DIA-MS, an approach that enables cross-experiment data extraction and quantitation for improved label-free statistical analysis. While this approach provides robust statistical power for label-free analysis, the data are likely inherently biased toward more abundant proteins or proteins with higher modification stoichiometry. In addition, thresholds applied to the hydroxylamine treatment dataset will group proteins that are palmitoylated along with proteins modified by multiple lipid acylations (e.g., palmitoylated and myristoylated).

Given that *T. gondii* is often described as a model organism for *P. falciparum* (Kim and Weiss, 2004), the limited overlap between the published palmitome for this related parasite and our dataset is surprising. This lack of overlap may be due to low homology between the species and subsequent difficulty in identifying orthologs in silico. However, the biology of these two organisms differs in many respects, and the lack of overlap may indicate that most palmitoylation is parasite specific. A good example of this is demonstrated here; TgAMA1 is palmitoylated, while PfAMA1 is not (Jones et al., 2012). Conversely, proteins that do overlap between datasets could represent evolutionarily conserved palmitoylation events.

Highlighting the critical role palmitoylation likely plays in the formation and/or function of the glideosome complex, we identified most components of the MyoA glideosome (MyoA, MLC1, GAP45, GAP40, and GAP50) within the MS dataset as palmitoylated protein species (Table S1). Moreover, a recent study investigating functional plasticity of glideosome components described an alternative, basally localized glideosome complex referred to as the MyoC glideosome (Frénal et al., 2014). Consistent with the underlying functional significance of palmitoylation for the glideosome, our proteomic study identified GAP80 and IAP1, two components of the MyoC glideosome (Frénal et al., 2014) as highly hydroxylamine-sensitive hits. Notably, MyoC was absent from our data.

We have shown that AMA1 in *T. gondii* has a previously unidentified palmitoylation site. Although AMA1 has been implicated in attachment and/or invasion (Bargieri et al., 2013, 2014; Hehl et al., 2000; Lamarque et al., 2014; Mital et al., 2005; Tyler et al., 2011), parasites expressing the AMA1 palmitoylation site mutant invade normally. One phenotype associated with mutation of the AMA1 palmitolyation site is a marked increase in the secretion of AMA1 and other microneme proteins, suggesting a previously unrecognized role for AMA1 in regulating microneme secretion. We also observed that mutant parasites that remain extracellular for 4 hr prior to invasion are less likely to complete their lytic cycle. The biological relevance of this observation is unclear. It may reflect involvement of TgAMA1 in intracellular replication, which would be consistent with the previous suggestion that intramembrane cleavage of TgAMA1 triggers parasite replication (Santos et al., 2011). However, other work has shown that parasites expressing non-cleavable mutants of TgAMA1 (Parussini et al., 2012) or lacking AMA1 altogether (Bargieri et al., 2013) replicate indistinguishably from wild-type, as do parasites lacking the rhomboid proteases necessary for TgAMA1 intramembrane cleavage (Rugarabamu et al., 2015; Shen et al., 2014), casting doubt on the connection between TgAMA1 cleavage and replication initiation. Palmitoylation of AMA1 could instead be involved in some previously unidentified function of the protein, such as fission of the parasitophorous vacuole membrane from the host cell plasma membrane during the final stages of invasion, although this would not explain why the phenotype only manifests after the parasites have been extracellular for 4 hr. It could be that enhanced secretion of microneme proteins in AMA1^{C504S} parasites while extracellular exhausts them of a protein normally secreted from the micronemes intracellularly, which is needed to complete the lytic cycle. Further studies will be required to test the hypothesis that

microneme secretion occurs intracellularly and plays a role in the parasite's lytic cycle. Finally, it is formally possible that phenotypes observed are not a direct consequence of the mutation introduced into AMA1, but rather a compensatory change induced by the mutation (Frénal and Soldati-Favre, 2015) such as downregulated expression of AMA2 (Figure S4A).

Recent studies dissecting the function of AMA1 cleavage from the surface of the parasite by the rhomboid proteases ROM4 and ROM5 have determined that the bulk of AMA1 is cleaved by ROM4, with a small proportion cleaved by ROM5 (Rugarabamu et al., 2015; Shen et al., 2014). Our data indicate that ROM4 is palmitoylated, and so palmitoylation could be a mechanism to organize enzyme and substrate. Furthermore, Rugarabamu and colleagues suggest that "The restricted access of ROM5 to a large pool of AMA1 is plausibly due to distinct lipid microenvironment or more likely as a result of compartmentalization," (Rugarabamu et al., 2015). It is intriguing to speculate that when AMA1 is not palmitoylated a greater proportion of the pool can be accessed by ROM5 and that the shift in the pools of the AMA1 accessed by ROM4 and ROM5 functionally contributes to the phenotypes observed herein.

In conclusion, we have generated a dataset that implicates palmitoylation in distinct aspects of *Toxoplasma* biology and have validated the palmitoylation of several proteins. In the case of extensively studied TgAMA1, we have shown that mutation of the likely palmitoylation site has no effect on invasion but causes a marked increase in microneme secretion, suggesting a role for AMA1 in this process. We have shown that this dataset can unlock unexpected biology for even the most well-studied proteins and will be a powerful resource for the future.

EXPERIMENTAL PROCEDURES

Labeling with 17-ODYA and Palmitic Acid

Parasites were labeled overnight (~16 hr) in culture medium with 25 μM palmitic acid or 25 μM 17-ODYA. Parasites were isolated by syringe lysis from HFFs, spun at 1200 × *g* for 5 min to remove host cell debris. Intracellular parasites were labeled as described, with infected host cells scraped, spun down, and washed in PBS to collect intracellular parasites.

Validation of Palmitoylation

Labeled parasites were lysed by sonication in 1× PBS with 10 μM PMSF and 20 μM HDSF. Membranes were pelleted by centrifugation at 100,000 × *g* for 1 hr at 4°C. Protein concentration was assessed by BCA. GFP IP setup was as follows: 60 μl of GFP-TRAP A beads from Chromotek were incubated with 200 μg of membrane lysate and IP buffer (150 mM NaCl, 20 mM HEPES [pH 7.4], 0.1% SDS, 0.5% NP40) for a total volume of 200 μl. IPs were incubated overnight at 4°C, then washed 3× with cold IP buffer, 2× with cold wash buffer (150 mM NaCl, 20 mM HEPES [pH 7.4]), and once with cold 1× PBS. Beads were resuspended in a 50 μl click reaction (1 mM $CuSO_4$, 1 mM TCEP, 100 μM Tris[(1-benzyl-1H-1,2,3-triazol-4-yl)methyl]amine [ligand], and 20 μM Azido-Rhodamine in 1× PBS). Reactions were incubated for 1 hr at 23°C, then split in half. NH_2OH (5% of total) was added to half of the reaction and incubated for 30 min at 23°C. Protein was eluted from beads by boiling in sample buffer and separated by SDS-PAGE. FLAG IPs were performed as for GFP, using 60 μl Sigma anti-FLAG M2 affinity gel. Gels were scanned on an Amersham Bioscience Typhoon 9410 variable mode imager using the 580 bp Filter with the green 532 laser. Gels were transferred to nitrocellulose and westerns performed to confirm IP of protein of interest. Western blots for AMA1 were performed using UVT-59 (Donahue et al., 2000), for TgMLC1 using anti-TgMLC1, for FLAG using anti-FLAG M2 (Sigma), and for GFP using the GF28R (Thermo Scientific) antibody.

For inputs, 50 μg of membrane lysate were added to a 50 μl click reaction described above. Reactions were incubated for 1 hr at 23°C and boiled in sample buffer. 5 μg were loaded for each input.

Invasion and Plaque Assays

Laser scanning cytometer-based invasion assays were done as previously described (Mital et al., 2005), with the following modifications: (a) the parasites were allowed to settle onto the HFF monolayers for 20 min at 23°C before incubation at 37°C for 1 hr; and anti-SAG1 primary, RPE-conjugated secondary, and Alexa 647-conjugated secondary antibodies were used at dilutions of 1:250, 1:400, and 1:200, respectively. A total of three biological replicates (each done in duplicate) were performed; Student's t test was applied to the means of the biological replicates.

Plaque assays were set up immediately following the initiation of invasion assays, using the same parasite suspensions. Fifty parasites were added to each well of a 12-well plate containing confluent host cell HFF monolayers. The plate was incubated for 7 days in the 37°C incubator with 5% CO_2 and humidity, then stained with 2% crystal violet and 20% methanol in PBS for 5 min at 23°C. The stained wells were washed with water, and the number of plaques per well were counted.

Replication Assay

WT and C504S parasites were harvested and allowed to sit at 23°C for 4 hr in DMEM with 1% FBS. Parasites were counted, and 5 × 10^5 parasites were added to 25 mm coverslips with confluent human foreskin fibroblasts. After 14 hr, coverslips were fixed on ice with 100% cold methanol for 5 min. Indirect IFAs were performed using anti-GRA8 and anti-GAP45 antibodies as previously described (Carey et al., 2000). A total of three biological replicates were performed with triplicates in each, and 250 vacuoles were counted per coverslip. Two-way ANOVA with Sidak's multiple comparisons test was performed.

Additional details can be found in the Supplemental Information.

SUPPLEMENTAL INFORMATION

Supplemental Information includes Supplemental Experimental Procedures, four figures, and two tables and can be found with this article online at http://dx.doi.org/10.1016/j.chom.2015.09.006.

AUTHOR CONTRIBUTIONS

I.T.F., M.A.C., and S.K. performed experiments. B.R.M. prepared samples for mass spectrometry. J.D.M. performed mass spectrometry, and data were analyzed by B.R.M. and J.D.M. W.A.v.d.L. generated 17-ODYA. I.T.F., M.A.C., S.K., J.D.M., G.E.W., B.R.M., and M.B. developed experimental plans, analyzed data, and wrote the paper.

ACKNOWLEDGMENTS

We would like to thank past and present Bogyo and Ward, and Martin lab members. This work was funded by the following: American Heart Association 14POST20280004 and NIH training grant 5T32AI007328 (I.T.F.); NIH Grants R01GM111703 (M.B.), R01AI063276 (G.E.W.), and DP2GM114848 and R00CA151460 (B.R.M.); American Heart Association 14POST20420040 and the University of Michigan (J.D.M.); and The Netherlands Organization for Scientific Research (NWO) Rubicon fellowship (W.A.v.d.L.).

Received: June 17, 2015
Revised: August 25, 2015
Accepted: September 16, 2015
Published: October 14, 2015

REFERENCES

Alonso, A.M., Coceres, V.M., De Napoli, M.G., Nieto Guil, A.F., Angel, S.O., and Corvi, M.M. (2012). Protein palmitoylation inhibition by 2-bromopalmitate alters gliding, host cell invasion and parasite morphology in Toxoplasma gondii. Mol. Biochem. Parasitol. *184*, 39–43.

Bargieri, D.Y., Andenmatten, N., Lagal, V., Thiberge, S., Whitelaw, J.A., Tardieux, I., Meissner, M., and Ménard, R. (2013). Apical membrane antigen 1 mediates apicomplexan parasite attachment but is dispensable for host cell invasion. Nat. Commun. *4*, 2552.

Bargieri, D., Lagal, V., Andenmatten, N., Tardieux, I., Meissner, M., and Ménard, R. (2014). Host cell invasion by apicomplexan parasites: the junction conundrum. PLoS Pathog. *10*, e1004273.

Barkhuff, W.D., Gilk, S.D., Whitmarsh, R., Tilley, L.D., Hunter, C., and Ward, G.E. (2011). Targeted disruption of TgPhIL1 in Toxoplasma gondii results in altered parasite morphology and fitness. PLoS ONE *6*, e23977.

Beck, J.R., Rodriguez-Fernandez, I.A., de Leon, J.C., Huynh, M.H., Carruthers, V.B., Morrissette, N.S., and Bradley, P.J. (2010). A novel family of Toxoplasma IMC proteins displays a hierarchical organization and functions in coordinating parasite division. PLoS Pathog. *6*, e1001094.

Beck, J.R., Fung, C., Straub, K.W., Coppens, I., Vashisht, A.A., Wohlschlegel, J.A., and Bradley, P.J. (2013). A Toxoplasma palmitoyl acyl transferase and the palmitoylated armadillo repeat protein TgARO govern apical rhoptry tethering and reveal a critical role for the rhoptries in host cell invasion but not egress. PLoS Pathog. *9*, e1003162.

Binder, E.M., Lagal, V., and Kim, K. (2008). The prodomain of Toxoplasma gondii GPI-anchored subtilase TgSUB1 mediates its targeting to micronemes. Traffic *9*, 1485–1496.

Black, M.W., and Boothroyd, J.C. (2000). Lytic cycle of Toxoplasma gondii. Microbiol. Mol. Biol. Rev. *64*, 607–623.

Carey, K.L., Donahue, C.G., and Ward, G.E. (2000). Identification and molecular characterization of GRA8, a novel, proline-rich, dense granule protein of Toxoplasma gondii. Mol. Biochem. Parasitol. *105*, 25–37.

Charollais, J., and Van Der Goot, F.G. (2009). Palmitoylation of membrane proteins (Review). Mol. Membr. Biol. *26*, 55–66.

Chaudhary, K., Donald, R.G., Nishi, M., Carter, D., Ullman, B., and Roos, D.S. (2005). Differential localization of alternatively spliced hypoxanthine-xanthine-guanine phosphoribosyltransferase isoforms in Toxoplasma gondii. J. Biol. Chem. *280*, 22053–22059.

Che, F.Y., Madrid-Aliste, C., Burd, B., Zhang, H., Nieves, E., Kim, K., Fiser, A., Angeletti, R.H., and Weiss, L.M. (2011). Comprehensive proteomic analysis of membrane proteins in Toxoplasma gondii. Mol. Cell. Proteomics *10*, 000745.

Child, M.A., Hall, C.I., Beck, J.R., Ofori, L.O., Albrow, V.E., Garland, M., Bowyer, P.W., Bradley, P.J., Powers, J.C., Boothroyd, J.C., et al. (2013). Small-molecule inhibition of a depalmitoylase enhances Toxoplasma host-cell invasion. Nat. Chem. Biol. *9*, 651–656.

Crawford, J., Tonkin, M.L., Grujic, O., and Boulanger, M.J. (2010). Structural characterization of apical membrane antigen 1 (AMA1) from Toxoplasma gondii. J. Biol. Chem. *285*, 15644–15652.

De Napoli, M.G., de Miguel, N., Lebrun, M., Moreno, S.N., Angel, S.O., and Corvi, M.M. (2013). N-terminal palmitoylation is required for Toxoplasma gondii HSP20 inner membrane complex localization. Biochim. Biophys. Acta *1833*, 1329–1337.

Distler, U., Kuharev, J., Navarro, P., Levin, Y., Schild, H., and Tenzer, S. (2014). Drift time-specific collision energies enable deep-coverage data-independent acquisition proteomics. Nat. Methods *11*, 167–170.

Donahue, C.G., Carruthers, V.B., Gilk, S.D., and Ward, G.E. (2000). The Toxoplasma homolog of Plasmodium apical membrane antigen-1 (AMA-1) is a microneme protein secreted in response to elevated intracellular calcium levels. Mol. Biochem. Parasitol. *111*, 15–30.

Frénal, K., and Soldati-Favre, D. (2015). Plasticity and Redundancy in Proteins Important for Toxoplasma Invasion. PLoS Pathog. *11*, e1005069.

Frénal, K., Polonais, V., Marq, J.B., Stratmann, R., Limenitakis, J., and Soldati-Favre, D. (2010). Functional dissection of the apicomplexan glideosome molecular architecture. Cell Host Microbe *8*, 343–357.

Frénal, K., Tay, C.L., Mueller, C., Bushell, E.S., Jia, Y., Graindorge, A., Billker, O., Rayner, J.C., and Soldati-Favre, D. (2013). Global analysis of apicomplexan protein S-acyl transferases reveals an enzyme essential for invasion. Traffic *14*, 895–911.

Frénal, K., Marq, J.B., Jacot, D., Polonais, V., and Soldati-Favre, D. (2014). Plasticity between MyoC- and MyoA-glideosomes: an example of functional compensation in Toxoplasma gondii invasion. PLoS Pathog. *10*, e1004504.

Fung, C., Beck, J.R., Robertson, S.D., Gubbels, M.J., and Bradley, P.J. (2012). Toxoplasma ISP4 is a central IMC sub-compartment protein whose localization depends on palmitoylation but not myristoylation. Mol. Biochem. Parasitol. *184*, 99–108.

Garrison, E., Treeck, M., Ehret, E., Butz, H., Garbuz, T., Oswald, B.P., Settles, M., Boothroyd, J., and Arrizabalaga, G. (2012). A forward genetic screen reveals that calcium-dependent protein kinase 3 regulates egress in Toxoplasma. PLoS Pathog. *8*, e1003049.

Gaskins, E., Gilk, S., DeVore, N., Mann, T., Ward, G., and Beckers, C. (2004). Identification of the membrane receptor of a class XIV myosin in Toxoplasma gondii. J. Cell Biol. *165*, 383–393.

Gilk, S.D., Raviv, Y., Hu, K., Murray, J.M., Beckers, C.J., and Ward, G.E. (2006). Identification of PhIL1, a novel cytoskeletal protein of the Toxoplasma gondii pellicle, through photosensitized labeling with 5-[125I] iodonaphthalene-1-azide. Eukaryot. Cell *5*, 1622–1634.

Hang, H.C., Geutjes, E.J., Grotenbreg, G., Pollington, A.M., Bijlmakers, M.J., and Ploegh, H.L. (2007). Chemical probes for the rapid detection of Fatty-acylated proteins in Mammalian cells. J. Am. Chem. Soc. *129*, 2744–2745.

Hannoush, R.N., and Arenas-Ramirez, N. (2009). Imaging the lipidome: omega-alkynyl fatty acids for detection and cellular visualization of lipid-modified proteins. ACS Chem. Biol. *4*, 581–587.

Heal, W.P., Wickramasinghe, S.R., Bowyer, P.W., Holder, A.A., Smith, D.F., Leatherbarrow, R.J., and Tate, E.W. (2008). Site-specific N-terminal labelling of proteins in vitro and in vivo using N-myristoyl transferase and bioorthogonal ligation chemistry. Chem. Commun. (Camb.) (4), 480–482.

Hehl, A.B., Lekutis, C., Grigg, M.E., Bradley, P.J., Dubremetz, J.F., Ortega-Barria, E., and Boothroyd, J.C. (2000). Toxoplasma gondii homologue of plasmodium apical membrane antigen 1 is involved in invasion of host cells. Infect. Immun. *68*, 7078–7086.

Herm-Götz, A., Weiss, S., Stratmann, R., Fujita-Becker, S., Ruff, C., Meyhöfer, E., Soldati, T., Manstein, D.J., Geeves, M.A., and Soldati, D. (2002). Toxoplasma gondii myosin A and its light chain: a fast, single-headed, plus-end-directed motor. EMBO J. *21*, 2149–2158.

Jones, M.L., Collins, M.O., Goulding, D., Choudhary, J.S., and Rayner, J.C. (2012). Analysis of protein palmitoylation reveals a pervasive role in Plasmodium development and pathogenesis. Cell Host Microbe *12*, 246–258.

Kemp, L.E., Rusch, M., Adibekian, A., Bullen, H.E., Graindorge, A., Freymond, C., Rottmann, M., Braun-Breton, C., Baumeister, S., Porfetye, A.T., et al. (2013). Characterization of a serine hydrolase targeted by acyl-protein thioesterase inhibitors in Toxoplasma gondii. J. Biol. Chem. *288*, 27002–27018.

Kim, K., and Weiss, L.M. (2004). Toxoplasma gondii: the model apicomplexan. Int. J. Parasitol. *34*, 423–432.

Kostiuk, M.A., Corvi, M.M., Keller, B.O., Plummer, G., Prescher, J.A., Hangauer, M.J., Bertozzi, C.R., Rajaiah, G., Falck, J.R., and Berthiaume, L.G. (2008). Identification of palmitoylated mitochondrial proteins using a bio-orthogonal azido-palmitate analogue. FASEB J. *22*, 721–732.

Lamarque, M.H., Roques, M., Kong-Hap, M., Tonkin, M.L., Rugarabamu, G., Marq, J.B., Penarete-Vargas, D.M., Boulanger, M.J., Soldati-Favre, D., and Lebrun, M. (2014). Plasticity and redundancy among AMA-RON pairs ensure host cell entry of Toxoplasma parasites. Nat. Commun. *5*, 4098.

Leung, J.M., Tran, F., Pathak, R.B., Poupart, S., Heaslip, A.T., Ballif, B.A., Westwood, N.J., and Ward, G.E. (2014). Identification of T. gondii myosin light chain-1 as a direct target of TachypleginA-2, a small-molecule inhibitor of parasite motility and invasion. PLoS ONE *9*, e98056.

Linder, M.E., and Deschenes, R.J. (2007). Palmitoylation: policing protein stability and traffic. Nat. Rev. Mol. Cell Biol. *8*, 74–84.

Lourido, S., Tang, K., and Sibley, L.D. (2012). Distinct signalling pathways control Toxoplasma egress and host-cell invasion. EMBO J. *31*, 4524–4534.

Martin, B.R., and Cravatt, B.F. (2009). Large-scale profiling of protein palmitoylation in mammalian cells. Nat. Methods *6*, 135–138.

Martin, B.R., Wang, C., Adibekian, A., Tully, S.E., and Cravatt, B.F. (2012). Global profiling of dynamic protein palmitoylation. Nat. Methods *9*, 84–89.

McCoy, J.M., Whitehead, L., van Dooren, G.G., and Tonkin, C.J. (2012). TgCDPK3 regulates calcium-dependent egress of Toxoplasma gondii from host cells. PLoS Pathog. *8*, e1003066.

Meissner, M., Schlüter, D., and Soldati, D. (2002). Role of Toxoplasma gondii myosin A in powering parasite gliding and host cell invasion. Science *298*, 837–840.

Mital, J., Meissner, M., Soldati, D., and Ward, G.E. (2005). Conditional expression of Toxoplasma gondii apical membrane antigen-1 (TgAMA1) demonstrates that TgAMA1 plays a critical role in host cell invasion. Mol. Biol. Cell *16*, 4341–4349.

Montoya, J.G., and Liesenfeld, O. (2004). Toxoplasmosis. Lancet *363*, 1965–1976.

Mueller, C., Klages, N., Jacot, D., Santos, J.M., Cabrera, A., Gilberger, T.W., Dubremetz, J.F., and Soldati-Favre, D. (2013). The Toxoplasma protein ARO mediates the apical positioning of rhoptry organelles, a prerequisite for host cell invasion. Cell Host Microbe *13*, 289–301.

Parussini, F., Tang, Q., Moin, S.M., Mital, J., Urban, S., and Ward, G.E. (2012). Intramembrane proteolysis of Toxoplasma apical membrane antigen 1 facilitates host-cell invasion but is dispensable for replication. Proc. Natl. Acad. Sci. USA *109*, 7463–7468.

Polonais, V., Javier Foth, B., Chinthalapudi, K., Marq, J.B., Manstein, D.J., Soldati-Favre, D., and Frénal, K. (2011). Unusual anchor of a motor complex (MyoD-MLC2) to the plasma membrane of Toxoplasma gondii. Traffic *12*, 287–300.

Ren, J., Wen, L., Gao, X., Jin, C., Xue, Y., and Yao, X. (2008). CSS-Palm 2.0: an updated software for palmitoylation sites prediction. Protein Eng. Des. Sel. *21*, 639–644.

Robert-Gangneux, F., and Dardé, M.L. (2012). Epidemiology of and diagnostic strategies for toxoplasmosis. Clin. Microbiol. Rev. *25*, 264–296.

Rugarabamu, G., Marq, J.B., Guérin, A., Lebrun, M., and Soldati-Favre, D. (2015). Distinct contribution of Toxoplasma gondii rhomboid proteases 4 and 5 to micronemal protein protease 1 activity during invasion. Mol. Microbiol. *97*, 244–262.

Salaun, C., Greaves, J., and Chamberlain, L.H. (2010). The intracellular dynamic of protein palmitoylation. J. Cell Biol. *191*, 1229–1238.

Santos, J.M., Ferguson, D.J., Blackman, M.J., and Soldati-Favre, D. (2011). Intramembrane cleavage of AMA1 triggers Toxoplasma to switch from an invasive to a replicative mode. Science *331*, 473–477.

Shen, B., Buguliskis, J.S., Lee, T.D., and Sibley, L.D. (2014). Functional analysis of rhomboid proteases during Toxoplasma invasion. MBio *5*, e01795–e14.

Tang, Q., Andenmatten, N., Hortua Triana, M.A., Deng, B., Meissner, M., Moreno, S.N., Ballif, B.A., and Ward, G.E. (2014). Calcium-dependent phosphorylation alters class XIVa myosin function in the protozoan parasite Toxoplasma gondii. Mol. Biol. Cell *25*, 2579–2591.

Tom, C.T., and Martin, B.R. (2013). Fat chance! Getting a grip on a slippery modification. ACS Chem. Biol. *8*, 46–57.

Tyler, J.S., Treeck, M., and Boothroyd, J.C. (2011). Focus on the ringleader: the role of AMA1 in apicomplexan invasion and replication. Trends Parasitol. *27*, 410–420.

Zou, C., Ellis, B.M., Smith, R.M., Chen, B.B., Zhao, Y., and Mallampalli, R.K. (2011). Acyl-CoA:lysophosphatidylcholine acyltransferase I (Lpcat1) catalyzes histone protein O-palmitoylation to regulate mRNA synthesis. J. Biol. Chem. *286*, 28019–28025.